ACTA TECHNICA CORVINIENSIS
– Bulletin of Engineering
Tome X [2017]
Fascicule 3 [July – September]
ISSN: 2067 – 3809

[1, 2] Fatai O. ARAMIDE, [1] Idris B. AKINTUNDE

EFFECTS OF SILICON CARBIDE AND SINTERING TEMPERATURE ON THE PROPERTIES OF SINTERED MULLITE-CARBON COMPOSITE SYNTHESIZED FROM OKPELLA KAOLIN

[1] Department of Metallurgical and Materials Engineering, Federal University of Technology, Akure, NIGERIA
[2] African Materials Science and Engineering Network, (AMSEN) a Subsidiary of Regional Initiative for Science Education (RISE)

Abstract: The effects of the addition of silicon carbide and sintering temperatures on the physical and mechanical properties of sintered ceramic composite produced from kaolin and graphite was investigated. The kaolin and graphite of known mineralogical composition were thoroughly blended with 4 and 8 (vol.) % silicon carbide. From the homogeneous mixture of kaolin, graphite and silicon carbide, standard samples were prepared via uniaxial compaction. The test samples produced were subjected to firing (sintering) at 1300˚C, 1400˚C and 1500˚C. It was observed that increase in sintering temperature beyond 1400°C generally lead to reduced porosity of the samples; high contents of silicon carbide especially at temperature from and above 1400°C lead to higher porosity; cold crushing strength of samples with 4% SiC is seen to be better than those of samples with 8% SiC within sintering the temperature range of 1400°C and 1500°C; modulus of elasticity of both samples reached the maxima values at 1400°C but those of samples with 8% SiC is seen to be higher within the sintering temperature range of 1400°C and 1500°C; absorbed energy of both samples generally increased with increased sintering temperature; oxidation indices for both samples reach the maxima at the temperature of 1400°C but the resistance to oxidation is better for samples with 4% SiC within the sintering temperature range of 1400°C and 1500°C. It was concluded that samples with 4% SiC at the sintering temperature of 1400°C exhibit better property and is considered to be optimum.

Keywords: silicon carbide; mullite; graphite; sintering temperatures; phases

INTRODUCTION

Mullite is an important aluminum silicate ceramics; it is the only stable intermediate specie in the system SiO_2-Al_2O_3, which has the composition of $3Al_2O_3.2SiO_2$, corresponding to 71.8wt%. Its importance in technology together with its rareness in nature necessitates its synthesis. (Schneider et al. 2008; Schneider & Komarneni, 2005, Vieira et al. 2007) [1-3].

Many researchers have worked on mullite based ceramic composite.

Aramide et al. (2014) [4] reported on high temperature synthesis of zircon-mullite-zirconia refractory ceramic composite from clay based materials. They synthesized mullite within the matrix of zirconia using kaolinitic clay sourced from southwest Nigeria. The zircon component of the ceramic composite was formed through solid state reaction of silica content of the clay/excess silica from the process of mullitization. Moreover, Aramide et al. (2015) [5] reported on the in-situ synthesis of mullite fibers reinforced zircon-zirconia refractory ceramic composite from clay based materials. They investigated the effects of yttria and niobium oxide on the phase changes and mechanical properties of the samples they worked on. They concluded that the improved mechanical property of their samples was due to strengthening by both mullite fibers reinforcement and phase transformation strengthening.

Other researchers have also worked elaborately and reported their findings on mullite based/reinforced ceramic composites [6-8].

Zum Gahr [9] reported that if the microstructure is modified it could lead to reduction of the friction and the wear of alumina. Moreover, in 1996, he showed that by reducing the grain size of alumina and zirconia it will significantly decrease the wear [10].

Furthermore Dong et al [11], reported on the effects of additives like MgO, SiO_2, Fe_2O_3 and ZrO_2 on the mechanical and thermal properties of aluminum titanate ceramics. They concluded that the combined additives of MgO and Fe_2O_3 have an excellent improvement on the stability of aluminum titanate. Ebadzadeh and Ghasemi [12], reported that the addition of TiO_2 to mullite-ZrO_2 composites results into change of reaction sintering, densification and microstructure which alter the formation temperature and retention of t-ZrO_2 phase in these composites. Moya et al. [13] also reported that the microstructure of mullite-zirconia and alumina-zirconia composites can be modified by additives like CaO and MgO.

Aramide et al. [14] had synthesized mullite-carbon composite from the same materials without any additive. The objective of the present work is to examine the effects of sintering temperature and addition of silicon carbide on the phase evolutions of ceramic composite produced from kaolin and graphite.

MATERIALS AND METHODS

» Raw Materials

Clay sample used for this study (as mine Kaolin sample) was sourced from Okpella, Edo State southern part of Nigeria, Graphite and silicon carbide (SiC) were sourced from (Pascal Chemicals, Akure), this were used to maintain the granulometry of the mixture.

» Method

– Processing of raw materials (Graphite & Kaolin)

The raw materials (graphite and kaolin) were crushed into a coarse particle size, of about 10 mm for graphite and less than 2mm for kaolin; the crushed samples were further reduced by grinding using Herzog rod mill. The powdered samples were sieved using 600μm sizes aperture according to ASTM standards in an electric sieve shaker. The undersize that passed through the 600μm sieve aperture were used in the samples making.

– Phase and Mineralogical Composition of Raw kaolin and Graphite Electrode

The kaolin clay and graphite samples were carefully prepared for these analyses by digesting in reagents as described by Nabil and Barbara, (2012)[15]. The mineralogical phases present in the samples were determined using X-ray diffractometry (XRD). The phases are reported in Table 1.

» Experimental Procedure

– Composition calculation using the Rule of Mixtures Technique

Rule of Mixtures is a method of approach to approximate estimation of composite material properties, based on an assumption that a composite property is the volume weighed average of the phases (matrix and dispersed phase). According to Rule of Mixtures [Surappa, (2003)][15] the density of composite materials are estimated as follows:

$$\rho_{mixture} = W_{tf\ kaolin} \times \rho_{\ kaolin} + W_{tf.graphite} \times \rho_{graphite} \quad (1)$$

$$M_{mixture} = \rho_{mixture} \times vol._{\ mould}. \quad (2)$$

Where: $\rho_{mixture}$ represent density of the mixture, $M_{mixture}$ is the mass of the mixture, $W_{tf.\ kaolin}$ is the weight fraction of kaolin, ρ_{kaolin} is the density of kaolin, $W_{tf.graphite}$ is the weight fraction of graphite, $\rho_{graphite}$ is the density of graphite and $vol._{mould}$ is volume of mould.

– Composites Production

The raw materials in the samples making were 3:2 vol. % of kaolin and graphite respectively with the addition of 4 and 8 (vol.) % silicon carbide respectively. The mixture were blended thoroughly for proper distribution of constituents materials in a ball mill for 3 hours at a speed of 72 rev/min after weighing via electronic weighing balance in accordance with the composition calculation initially prepared [Aramide et al. (2014); Aramide, (2015)][17, 18].

The resulting blended compositions were mixed with 10% water of kaolin content in each composition; this was in order to enhance the plasticity of the mixture during compaction. The mixed samples were subjected to uniaxial compaction, which was carried out mechanically under pressure. The moulded materials were fired at varying temperatures (1300°C, 1400°C and 1500°C). After which the samples were subjected to various test, to examine the phase analysis, evaluate their physical and mechanical properties.

» Testing

– Shrinkage Measurement

The shrinkage properties of the pressed samples were determined by measuring both the green and fired dimensions, using a digital vernier caliper. The thickness and diameters were measured for evaluation and computation of the shrinkage [Aramide, (2015)][18].

$$\%\ \text{linear shrinkage} = \frac{(Lg-Lf)}{(Lg)} \times 100 \quad (3)$$

$$\%\ \text{volumetric shrinkage} = \frac{(Vg-Vf)}{(Vg)} \times 100 \quad (4)$$

where: Lg represent the green length and Lf represent the fired length; Vg represent the green volume and Vf represent the fired Volume

– Apparent porosity (AP)

Test samples from each of the ceramic composite samples were dried out for 12 hours at 110°C. The dry weight of each fired sample was taken and recorded as D. Each sample was immersed in water for 6 hours to soak and weighed while being suspended in air. The weight was recorded as W.

Finally, the specimen was weighed when immersed in water [Aramide et al. (2014); Aramide, (2015)][17, 18]. This was recorded as S. The apparent porosity was then calculated from the expression:

$$\%\ \text{apparent porosity} = \frac{(W-D)}{(W-S)}\ \text{x}\ 100 \qquad (5)$$

– Bulk Density

The test specimens were dried out at 110˚C for 12 hours to ensure total water loss. Their dry weights were measured and recorded. They were allowed to cool and then immersed in a beaker of water.

Bubbles were observed as the pores in the specimens were filled with water. Their soaked weights were measured and recorded. They were then suspended in a beaker one after the other using a sling and their respective suspended weights were measured and recorded [Aramide et al. (2014); Aramide, (2015)][17, 18]. Bulk densities of the samples were calculated using the formula below:

$$\text{Bulk density} = \frac{D}{(W-S)} \qquad (6)$$

where: D rep. Weight of dried specimen, S rep. Weight of dried specimen suspended in water, and W rep. Weight of soaked specimen suspended in air.

– Cold Compression Strength, Modulus of Elasticity and Absorbed Energy

Cold compression strength test is to determine the compression strength to failure of each sample, an indication of its probable performance under load. The standard ceramic samples were dried in an oven at a temperature of 110˚C, allowed to cool.

The cold compression strength tests were performed on INSTRON 1195 at a fixed crosshead speed of 10mm min^{-1}. Samples were prepared according to ASTM C133-97 (ASTM C133-97, 2003) [Aramide et al. (2014); Aramide, (2015)] [17, 18] cold crushing strength, modulus of elasticity and absorbed energy of standard and conditioned samples were calculated from the equation:

$$\text{CCS} = \frac{(\text{Load to fracture})}{(\text{Surface area of sample})} \qquad (7)$$

– Oxidation Resistance

The fired samples after heat-treatment were cut and the diameter of black portion was measured at different locations and the average value was taken. Lower oxidation index indicates the higher oxidation resistance of the sample [Kuldeep, (2014); Subham, (2013)] [19, 20]. Oxidation index is determined by the formula:

$$\text{Oxidation index} = \frac{(\text{Area of oxidized zone}}{\text{Total area})} \times 100 \qquad (8)$$

RESULTS AND DISCUSSION

Tables 1 and 2 with Figures 1 to 4 show the effects of sintering temperatures and silicon carbide additive on the various physical and mechanical properties of various samples. From the various figures, it is observed that both the sintering temperature and the varied percentage silicon carbide additive affect the investigated properties of the various samples.

» Phase/Mineralogical Composition of the Raw Kaolin and Graphite Samples

The phase/mineralogical composition of the kaolin and graphite samples were characterised (investigated) with the aid of X-ray diffractometer. The results of the phase analysis of kaolin and graphite powder quantified by XRD were presented in Table 1.

The discussion of the raw phase/mineralogical composition of the raw raw materials used is not within the scope of this article; they are only reported for the purpose of showing that the compositions of the starting raw materials were known.

Table 1. XRD Results of kaolin and graphite sample showing the quantity of different phases present

Materials	Kaolinite (wt. %)	Quartz (wt. %)	Amorphous wt. (%)	Graphite (wt. %)
Kaolin Sample	63.23	0.65	36.13	-
Graphite Sample	-	-	56.9	43.1

» Effects of sintering temperature and silicon carbide additive on the physical properties of the samples

Figures 1 and 2 show the effects of sintering temperature of the apparent porosity and bulk density of the various samples investigated.

– Effects of sintering temperature and silicon carbide additive on the apparent porosity of the samples

Figure 1 and Table 2 show the effects of sintering temperature and silicon carbide additives on the apparent porosity of the various investigated samples. From the figure, it is observed that for sample C1 (4 % silicon carbide) the apparent porosity slightly increased from 30.282% at 1300°C to 30.435% when the sintering temperature was increased to 1400°C.

Further increase in the sintering temperature to 1500°C leads to sharp reduction in the apparent porosity of the samples to 28.125%. Increase in sintering temperature is expected to lead to the densification of the sample [18]. The slight initial increase in the apparent porosity of the sample as the sintering temperature is increased from 1300°C to 1400°C is due to high temperature oxidation of graphite based ceramics [21].

The sharp reduction in the apparent porosity of the sample as the sintering temperature is increased to 1500°C could be attributed to the anti-oxidation effect of the silicon carbide additive. It is an established fact that silicon carbide undergoes mostly passive oxidation [22] which leads to liberation of silica. This silica forms dense layer on the surface of the graphite which acts as a protective barrier on the graphite against oxygen penetration [23]. This leads to the reduction of the apparent porosity as the dense layer of silica formed on the surface of the sample. This could also explain the reason for the linear expansion recorded in various samples instead of linear shrinkage.

Similarly, for sample C2 it is observed that its apparent porosity initially increased from 29.686% at 1300°C to 30.993% as the sintering temperature is increased to 1400°C. Further increase in the sintering temperature to 1500°C leads to slight reduction in the apparent porosity to 30.435%.

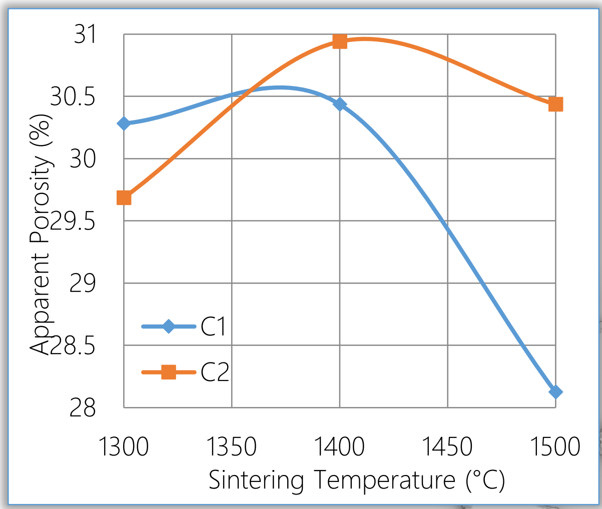

Figure 1. Effects of sintering temperature on the apparent porosity of the sample

It equally observed that sample C2 (8% silicon carbide) have higher apparent porosity than sample C1 (4% silicon carbide) at all sintering temperature with the exception of 1300°C.

- **Effects of sintering temperature and silicon carbide additive on the bulk density of the samples**

The effects of sintering temperature and silicon carbide additive on the bulk density of the investigated samples are depicted in Figure 2. From the figure, for sample C1 it is observed that the bulk density of the sample reduced from 1.655 g/cm³ at 1300°C to 1.619 g/cm³ when the sintering temperature was increased to 1400°C.

Further increase in the sintering temperature to 1500°C leads to increase in the bulk density of the sample to 1.699 g/cm³. This is expected following the behavior of the apparent porosity of the sample with the sintering temperature as discussed in the preceding section (Figure 1).

Since increased apparent porosity means that the sample is less dense, (that is, it contains less matter and more pores) [24] this is why the bulk density reduced while the apparent porosity increased and vice versa. For sample C2, it is observed that the bulk density of the sample reduced from 1.728 g/cm³ at 1300°C to 1.719 g/cm³ when the sintering temperature was increased to 1400°C. But it is observed that increased sintering temperature to 1500°C had no effect on the bulk density (it remains constant at 1.719 g/cm³). It is also observed that sample C2 possesses higher bulk density than sample C1 at all investigated temperature; this could be due to the density contribution of the silicon carbide additive, which is more in C2 than in C1.

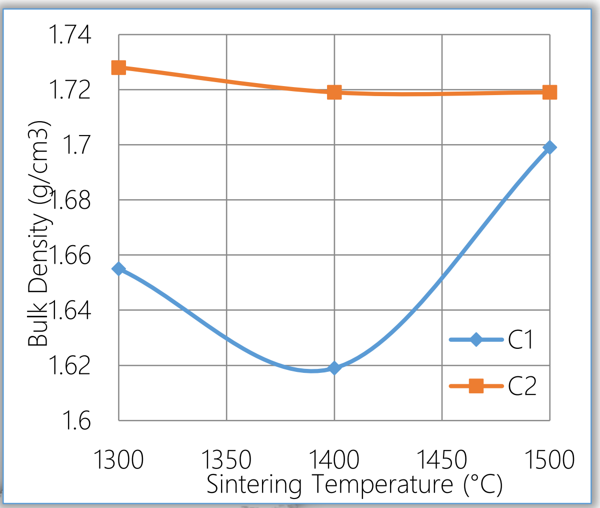

Figure 2. Effects of sintering temperature on the bulk density of the sample

- **Effects of sintering temperature and silicon carbide additive on the cold crushing strength of the samples**

Figure 3 depicts the effects of sintering temperature and silicon carbide additive on the cold crushing strength of the samples. From the figure, it is observed for sample C1 that the cold crushing strength at 1300°C was about 7.43 Mpa, it was observed to reduce to about 7.28 Mpa with increase in sintering temperature to 1400°C. Thereafter increased sintering temperature to 1500°C leads to increase in the cold crushing strength of the sample to about 7.53 Mpa.

It is observed that Figure 3 follows almost the same trend as Figure 2; higher cold crushing strength is observed where higher bulk density is observed and vice versa. This is because high bulk density is favoured by low porosity (fewer pores) which implies that more matters are available to bear more load [24]. From the same Figure 3, sample C2 is seen to follow the same trend with sample C1.

It is observed that at 1300°C the cold crushing strength of sample C2 is about 7.65 Mpa, increased sintering temperature leads to reduction in the cold crushing strength to about 6.91 Mpa. This is due to increased porosity of the sample within the same temperature range [24].

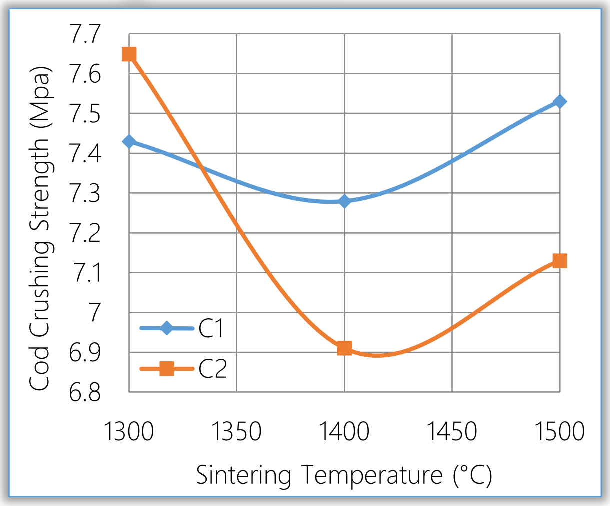

Figure 3. Effects of sintering temperature on the cold crushing strength of the samples

- **Effects of sintering temperature and silicon carbide additive on the modulus of elasticity of the samples**

Figure 4 shows the effects of sintering temperature and silicon carbide additive on the Young's modulus of elasticity of the investigated samples.

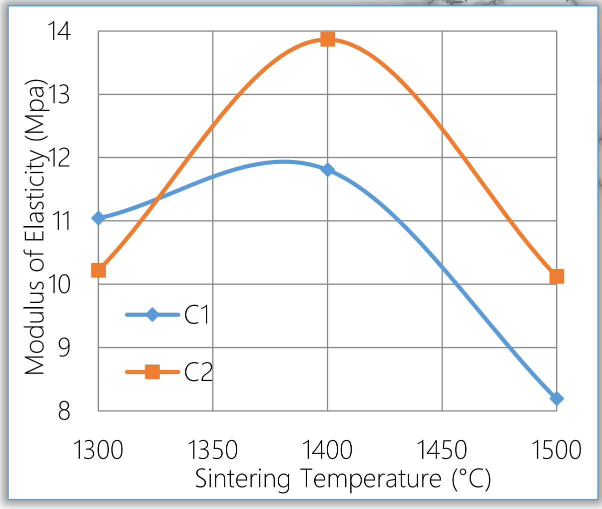

Figure 4. Effects of sintering temperature on the Young's modulus of elasticity of the samples

From the figure, it is observed that for sample C1 the modulus of elasticity of the sample initially at 1300°C is about 11.04 Mpa, it increased to about 11.81 Mpa (at 1400°C) with increased sintering temperature. The modulus of elasticity is observed to reduce to about 8.19 Mpa with further increased sintering temperature to 1500°C. Sample C2 is observed to follow the same trend with sample C1.

The modulus of elasticity of sample C2 at 1300°C was initially observed to be about 10.22 Mpa, it then increased to about 13.87 Mpa as the sintering temperature was increased to 1400°C. It is the observed to reduce to about 10.12 Mpa as the sintering temperature was further increased to 1500°C. Similar trend has been earlier reported by other researchers [25, 26] where it was reported that graphite does not improve the rigidity of refractory ceramic.

- **Effects of sintering temperature and silicon carbide additive on the absorbed energy of the samples**

Figure 5 depicts the effects of sintering temperature and silicon carbide additive on the absorbed energy of the investigated samples.

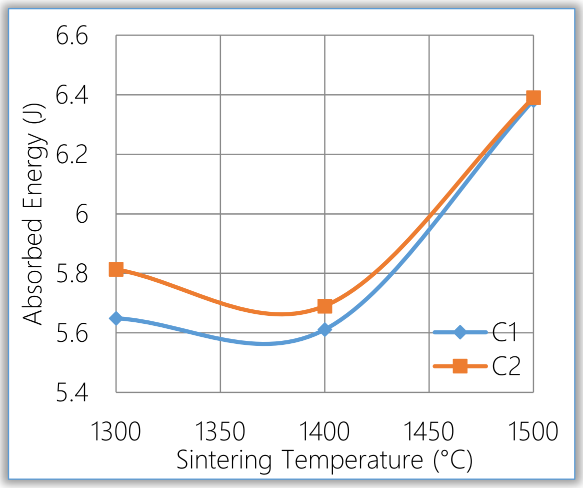

Figure 5. Effects of sintering temperature on the absorbed energy of the samples

From the figure, it is observed for sample C1 that the absorbed energy at 1300°C was about 5.65 J, this is seen to reduce slightly to about 5.61 J as the sintering temperature was increased to 1400°C; further increase in the sintering temperature to 1500°C leads to increase in the absorbed energy of the sample to about 6.38 J. Furthermore, it is observed from the figure that for sample C2, the absorbed energy's behavior with sintering temperature follows the same trend with that of sample C1 as earlier discussed.

Both samples having minima values for absorbed energy at 1400°C (as it was the case for both bulk density and cold crushing strength). Comparing this with Figure 1, it is observed that both samples C1 and C2 have their maxima values for apparent porosity at 1400°C. It is also observed that the absorbed energy of the sample C2 is greater than that of the sample C1 at all sintering temperatures.

- **Effects of sintering temperature and silicon carbide additive on the linear expansion of the samples**

The effect of sintering temperature and silicon carbide additive on the linear expansion of the investigated samples is depicted in Figure 6. It is observed for both samples C1 and C2 that the linear expansion increased from its lowest (for each of the investigated samples) at 1300°C to its maximum at 1400°C. It then reduced slightly with further increase in the sintering temperature to 1500°C. What is commonly observed in most ceramic is linear shrinkage, but contrary to the common linear shrinkage in the investigated samples, what is observed is linear expansion. This is due to the excess silica liberated during the process of mullitization on one hand, and the liberation of silica by the 'passive oxidation' of silicon carbide on the samples.

The silica forms dense layer on the surface of the samples which increased the length (diameter) of the samples [22]. It will be observed that the linear expansion values for sample C2 at 1300°C and 1400°C were greater than those of sample C1 at the same sintering temperature. This is because sample C2 contains 8 vol % of silicon carbide while sample C1 contains 4 vol % silicon carbide. On the contrary the linear expansion value of sample C1 at 1500°C is greater than that of sample C2. It equally observed that maxima linear expansion values both samples C1 and C2 are at 1400°C.

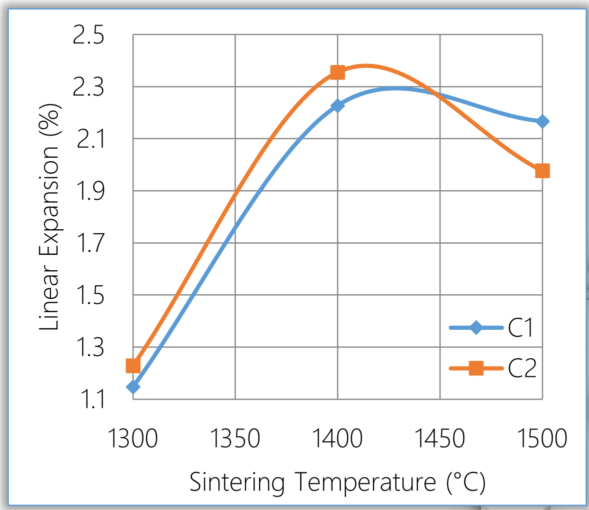

Figure 6. Effects of sintering temperature on the linear expansion on the samples

- **Effects of sintering temperature and silicon carbide additive on the volumetric shrinkage of the samples**

Figure 7 clearly depicts the effects of sintering temperature and silicon carbide on the volumetric shrinkage of the samples. From the figure it is observed that the volumetric shrinkages of both samples C1 and C2 initially reduced as the sintering temperature increased from 1300°C to 1400°C, reached the minima values at 1400°C and then increased with further increase in the sintering temperature to 1500°C. It is not a coincidence that both the minima volumetric shrinkage values and the maxima linear expansion values of both samples were observed at 1400°C. The silica that was liberated on the samples that lead to linear expansion was generated in situ and since matter can neither be created nor be destroyed, but can be transformed from one form to another. This means that the samples expand in two directions while they shrink in the third direction. This is why the volumetric shrinkage is observed in the samples.

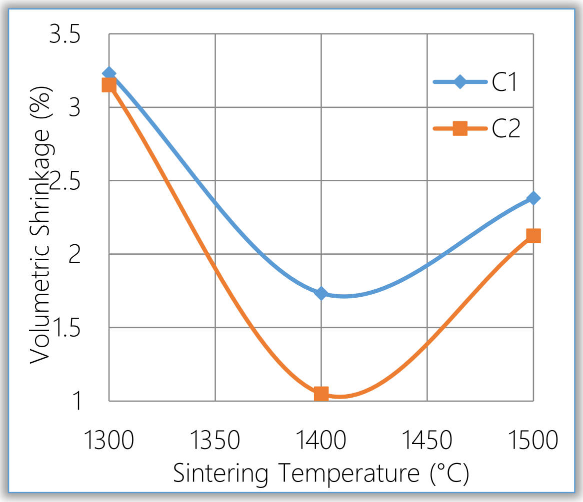

Figure 7. Effects of sintering temperature on the volumetric shrinkage of the samples

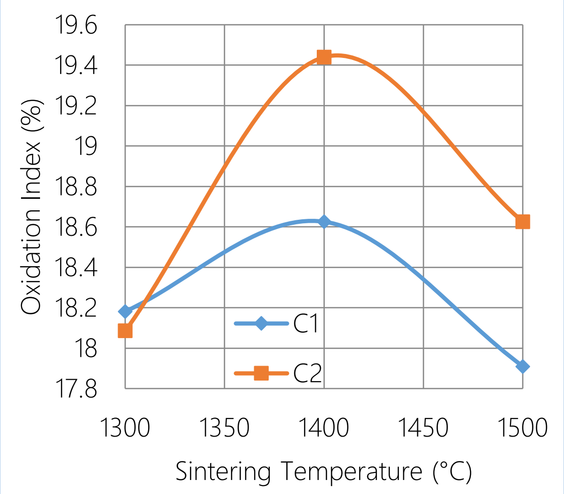

Figure 8. Effects of sintering temperature on the oxidation indices of the samples

- **Effects of sintering temperature and silicon carbide additive on the oxidation indices of the samples**

Figure 8 shows the effects of sintering temperature and silicon carbide additive on the oxidation indices of the samples. From the Figure, it is observed that the oxidation indices of the samples initially increased with increase in the sintering temperature from 1300°C to 1400°C. The oxidation index reached its maximum at 1400°C, further increase in the sintering temperature to 1500°C resulted into reduction in the oxidation indices for both samples C1 and C2. It has been earlier discussed that the reduction in the porosity of the samples as the sintering temperature is increased from 1400°C to 1500°C was due to the deposition of silica on the surface of the samples when silicon carbide was oxidized to form silica and carbon (graphite) [22, 23]. The silica formed filled up some of the pores. This shows that the silicon carbide acts as anti-oxidant for the graphite contents of the samples.

CONCLUSIONS

From the discussion of the data generated it is concluded that;

- increase in sintering temperature beyond 1400°C generally lead to reduced porosity of the samples;
- high contents of silicon carbide especially at temperature from and above 1400°C lead to higher porosity;
- high contents of silicon carbide lead to production of dense samples;
- cold crushing strength of sample C1 (4% SiC) is seen to be better than those of sample C2 (8% SiC) within sintering the temperature range of 1400°C and 1500°C;
- modulus of elasticity of both samples reached the maxima values at 1400°C but those of sample C2 (8% SiC) is to be higher within the sintering temperature range of 1400°C and 1500°C;
- absorbed energy of both samples generally increased with increased sintering temperature;
- oxidation indices for both samples reach the maxima at the temperature of 1400°C but the resistance to oxidation is better for sample C1 (4% SiC) within the sintering temperature range of 1400°C and 1500°C;
- sample C1 (4% SiC) at the sintering temperature of 1400°C is considered to exhibit better property and is considered to be optimum.

Acknowledgments

The authors acknowledge the Science Initiative Group (SIG), based at the Institute for Advanced Study in Princeton, for the support of this research work through the Competitive Fund for RISE Graduates Phase I (Round 1 and 3). Without this fund, it would have been extremely difficult to achieve the objectives of this research work.

Reference

[1.] Schneider H., Komanerni S. (2005) Mullite. Federal Republic of Germany.

[2.] chneider H., Schreuer J., Hildmann B. Structure and properties of mullite – A review, Journal European Ceramic Society, 2008, 28, 329-344.

[3.] Vieira S.C., Ramos A.S., Vieira M.T. Mullitization kinetics from silica and alumina-rich wastes. Ceramic international, 2007, 33, 59-66.

[4.] Aramide F.O., Alaneme K.K., Olubambi P.A., Borode J.O., High Temperature Synthesis of Zircon-Mullite-Zirconia Refractory Ceramic Composite from Clay Based Materials, in Volume 5 - Composite, Ceramic, Quasi-crystals, Nanomaterials & Coatings: 2014 – Sustainable Industrial Processing Summit & Exhibition/Shechtman International Symposium, held from 29 June - 04 July 2014, Fiesta Americana Condesa Cancun All Inclusive Resort, Cancun, Mexico, 2014, 155-176

[5.] Aramide F. O., Alaneme K. K., Olubambi P. A., Borode J. O., In-Situ Synthesis of Mullite Fibers Reinforced Zircon-Zirconia Refractory Ceramic Composite from Clay Based Materials, International Journal of Materials and Chemistry 2015; 5(6); 127-139.

[6.] Wen-Chang J. Wei, H. C. KaO and M. H. Lo, "Phase Transformation and Grain Coarsening of Zirconia-Mullite Composites" J. Europ. Ceram. Soc., 1996, 16, 239-247.

[7.] Maitra S., Pal S., Nath S, Pandey A., and Lodha R., "Role of MgO and Cr_2O_3 Additives on the Properties of Zirconia-Mullite Composites" Ceramics International, 2002, 28, 819-826.

[8.] Claussen N. and Ruhle M. "Design of Transformation-Toughned Ceramics" In. Science and Technology of Zirconia III, Advances in Ceramics, vol. 24, American Ceramics Society, OH, 1988, 137.

[9.] Zum Gahr, K.-H. Effect of grain size on friction and sliding wear of oxide ceramics, Wear 162–164, (1993) 269–279.

[10.] Zum Gahr, K.-H. Modeling and microstructural modification of alumina ceramic for improved tribological properties, Wear 200 (1996) 215–224.

[11.] Dong Xiu-zhen, Wang Yi-ming, Li Yue. Additives' effect on aluminium titanate ceramics [J]. China Ceramics, 2008, 44(1): 7–10.

[12.] Ebadzadeh, T. and Ghasemi, E. Effect of TiO_2 addition on the stability of t-ZrO_2 in mullite-ZrO_2 composites prepared from various starting materials, Ceramics International, 2002, 28, 447–450.

[13.] Moya, J.S; Miranzo, P. and Osendi, M.I. Influence of additives on the microstructural development of mullite-ZrO_2 and alumina-ZrO_2, Materials Science and Engineering, 1989, AI09, 139-145.

[14.] Aramide F.O., Akintunde I.B., Oyetunji A.,. Insitu Synthesis and Characterization of Mullite-Carbon Refractory Ceramic Composite from Okpella Kaolin and Graphite, Usak University Journal of Material Sciences, 2016, 25-42

[15.] Nabil, R. B. and Barbara, Z., Sample Preparation for Atomic Spectrometric Analysis: An overview. Advances in Applied science research, 2012; 3 (3); 1733-1737

[16.] Surappa, M.K., Aluminium Matrix Composites: Challenges and Opportunities; Sadhana, 28, Parts 1 & 2, 2003; 319-334.

[17.] Aramide F.O., Alaneme K.K., Olubambi P.A., Borode J.O., Effects of 0.2Y-9.8ZrO_2 Addition on the Mechanical Properties and Phase Development of Sintered Ceramic Produced from Ipetumodu Clay, ANNALS of Faculty Engineering Hunedoara – International Journal of Engineering, 2014; 7(4); 343-352.

[18.] Aramide, F. O., Effects of sintering temperature on the phase developments and mechanical properties ifon clay. Leonardo Journal of Sciences 2015; Issue 26; 67-82.

[19.] Singh, K., Specially Treated Graphite Fortified Alumina-Silicon Carbide-Carbon Refractories: Fabrication and Properties, Master of Technology

Thesis, Department of Ceramic Engineering National Institute of technology Rourkela, 2014; 17-40.

[20.] Mahato, S., Expanded graphite fortified magnesia-carbon refractories: fabrication and Properties, Master of Technology Thesis, Department of Ceramic Engineering National Institute of technology Rourkela, 2013; 11-24.

[21.] Zhang H.Y., Wang H.Q., Chen G.H., A New Kind of Conducting Filler- Graphite Nano sheets, Plastics, 2006; 35(4): 42-50.

[22.] Roy J., Chandra S., Das S., Maitra S., Oxidation Behaviour of Silicon Carbide- A Review, Rev. Adv. Mater. Sci. 2014; 38, 29-39.

[23.] Auweter-Kurtz M., Hilfer G., Habiger H., Yamawaki K., Yoshinaka T., Speckmann H.D. Investigation of oxidation protected C/C heat shield material in different plasma wind tunnels, Acta Astronau. 1999; 45, 93.

[24.] Aramide F. O., Production and Characterization of Porous Insulating Fired Bricks from Ifon Clay with Varied Sawdust Admixture, Journal of Minerals and Materials Characterization and Engineering, 2012, 11, 970-975

[25.] Aramide F. O. and Oke S. R. Production and characterization of clay bonded carbon refractory from carbonized palm kernel shell, Acta Tehnica Corviniensis – Bulletin of Engineering, 2014, Tome VII, Fascicule 4, 133-140.

[26.] Oke S.R., Talabi H.K., Olorunniwo O.E., Atanda P.O., Aramide F.O., Production and Characterization of Clay Bonded Carbon Refractory from Ifon Clay and Spent Graphite Electrode. International Journal of Metallurgical Engineering, 2015, 4(2): 33-39

ISSN:2067-3809

University POLITEHNICA Timisoara,
Faculty of Engineering Hunedoara,
5, Revolutiei, 331128, Hunedoara, ROMANIA
http://acta.fih.upt.ro